Chemical Engineering Journal 160 (2010) 715–722

Contents lists available at ScienceDirect

Chemical Engineering Journal

journal homepage: www.elsevier.com/locate/cej

Enhancement of methane combustion in microchannels: Effects of catalyst segmentation and cavities

Yueh-Heng Li[a], Guan-Bang Chen[b,*], Hung-Wei Hsu[c], Yei-Chin Chao[a,**]

[a] Department of Aeronautics and Astronautics, National Cheng Kung University, Tainan 701, Taiwan, ROC
[b] Center for Energy Technology and Strategy, National Cheng Kung University, No. 1, Ta-Hsueh Rd., Tainan 701, Taiwan, ROC
[c] Aerospace Science and Technology Research Center, National Cheng Kung University, Tainan 701, Taiwan, ROC

ARTICLE INFO

Article history:
Received 4 December 2009
Received in revised form 4 March 2010
Accepted 23 March 2010

Keywords:
Numerical simulation
Multi-segment catalyst
Cavity
Micro-reactor

ABSTRACT

This paper proposes a novel design concept for the enhancement of methane combustion in a microchannel that uses the combined effects of catalyst segmentation and cavities. The effects and combustion characteristics are evaluated using numerical simulation with detailed heterogeneous and homogeneous chemistries. The effects of a multi-segment catalyst and cavities on channel walls are examined and discussed in terms of various catalyst layouts, cavity dimensions, flow conditions, and reactor properties. In general, the chemical process of conventional catalytic combustion is a competition between hetero- and homogeneous reactions for fuel, oxygen, and radicals. The objective of using catalyst segmentation and cavities in a micro-reactor is to integrate the advantages of the hetero- and homogeneous reactions to enhance fuel conversion and to promote complete combustion in a confined distance. In this catalyst configuration, the pre-reaction of the heterogeneous reaction in an upstream catalyst segment can produce intermediate chemical radicals and catalytically induced exothermicity; the homogeneous reaction is subsequently induced and anchored in the cavity. Carbon monoxide is massively discharged after the homogeneous reaction due to incomplete combustion. The downstream catalyst segments strongly deplete carbon monoxide due to its high sticking coefficient on the platinum surface. Full methane conversion and complete combustion can thus be achieved in a short distance. Cavities can appreciably extend the stable operational range of the micro-reactor for a wide variety of inlet flows. Moreover, etching localized cavities in a small-scale system can further stabilize the flame, and cavities can serve as the heat source for reactions. These benefits of the proposed catalyst configuration can be applied in the design of a small-scale power/heating generator.

1. Introduction

In the expanding applications of micro-electronic mechanical systems (MEMS), traditional batteries, which are limited by size, weight, and power density, have failed to satisfy the increasing demand for smaller scale and higher density power sources [1]. There is increasing demand for a tiny but powerful energy source. Micro-scale combustors [2–4] are regarded as a viable solution for providing the power and energy density required for micropower systems. Hydrocarbon fuels provide energy storage of typically 45 MJ kg^{-1}, whereas the best currently available batteries (lithium-ion) provide only about 0.5 MJ kg^{-1}. Even at 10% conversion efficiency from thermal to electrical energy, the energy storage density of hydrocarbon fuels is over 10 times higher than that of batteries [5–7]. Other advantages of hydrocarbon fuels over conventional batteries include low cost, no memory effect, and instant rechargeability. In addition, the shelf life of chemical fuels is much longer than that of batteries. A micro-scale power device that could harness the chemical energy of hydrocarbon fuel would enable significant increases in the power output and endurance of micropower devices. Therefore, using the energy density of a hydrocarbon fuel in a micro-combustion process is an attractive technology for micro-scale power generation.

When the combustor volume is reduced, issues such as residence time, fluid mixing, thermal management, and wall quenching of gas-phase reactions become important. The fuel–air mixture residence time in a small-scale combustor may be less than the chemical time for a premixed combustion system, or less than the combined mixing and chemical time for a non-premixed flame, making complete combustion in the chamber a serious challenge

* Corresponding author. Tel.: +886 6 2757575x31450; fax: +886 6 2095913.
** Corresponding author at: Institute of Aeronautics & Astronautics, National Cheng Kung University, No. 1, Ta-Hsueh Rd., Tainan 701, Taiwan, ROC.
Tel.: +886 6 2757575x63690; fax: +886 6 2389940.
E-mail addresses: gbchen26@gmail.com (G.-B. Chen), ycchao@mail.ncku.edu.tw (Y.-C. Chao).

1385-8947/$ – see front matter.
doi:10.1016/j.cej.2010.03.057

[8]. Tailoring the fluid flow to stabilize the flame and to allow effective mixing of the cold reactants with the hot product gases is therefore critical for complete combustion in a micro-combustor and constitutes a fundamental micro-combustor design challenge [9].

Some strategies have been proposed to overcome these shortcomings encountered in the process of miniaturization, such as applying a heat-recuperating system in a combustor [10,11], utilizing quench-resistant fuels [12] to reduce the effects of heat and chemical radical loss to the wall, and applying catalytic combustion characteristics to enhance the reaction and to suppress radical depletion on the wall [13–15]. It is well known that the use of certain catalyst material enables the initiation and progress of combustion reactions even when the characteristic combustor dimension is smaller than the typical quenching distance of the fuel and the mixture composition is beyond the flammability limit. Pertinent catalyst and catalyst bed design can result in an intense reaction and an improvement in heat loss and radical depletion through the reactor.

Numerical simulation is a convenient and cost-effective approach for studying micro-combustion and its mechanisms. Maruta et al. [16] used numerical simulation to study the extinction limits in a micro-catalytic channel with multiple-step reactions. They showed that, for adiabatic walls, the equivalence ratio at the extinction limit decreased monotonically with increasing Reynolds number, while for non-adiabatic conditions, the extinction curve exhibited U-shaped dual-limit behavior due to heat loss and insufficient residence time compared to chemical time. Raimondeau et al. [17] performed numerical simulations of methane/air flame propagation in a straight tubular microchannel with detailed gas-phase chemistry. It was found that radial gradients and temperature discontinuity on the wall were negligible in very small reactors. The near-entrance heat loss and radical quench on the wall were key factors that control flame propagation inside the microchannels.

Norton and Vlachos [18] conducted a two-dimensional CFD simulation to analyze premixed methane/air flame stability in a micro-combustor that consisted of two parallel, infinitely wide, 1-cm long plates with a small separation distance. They studied the effects of micro-combustion dimensions, conductivity and thickness of the wall, external heat losses, and operation conditions on the combustion characteristics and flame stability. Norton and Vlachos [19] also reported CFD results on the micro-combustion stability of propane/air mixtures. Hua et al. [20] performed numerical simulations to study premixed hydrogen/air combustion in a series of chambers with various dimensions from millimeter to micrometer levels. Kaisare and Vlachos [21] discussed the appropriate reactor length, wall thickness, and reactor opening size for self-sustained homogeneous combustion in parallel plate channels. The optimum gap width of 600–1200 μm provides the largest operation range of self-sustained combustion. They also found that size effects are stronger for methane combustion than they are for propane combustion.

Most previous computational studies have dealt with hetero- and homogeneous reactions separately and have concentrated on the extinction limits and flame stabilities. The effects of catalytic walls on combustion characteristics inside microchannels are still not fully understood nor well documented. In addition, few studies have investigated the effect of catalyst layout in a micro-scale reactor. In the present study, a symmetric CFD model with detailed multiple-step gas-phase and surface phase reaction mechanisms is used to investigate the effects of the proposed design of catalyst segmentation and cavities on methane/air combustion performance in a catalytic microchannel.

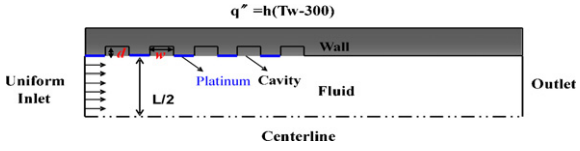

Fig. 1. Schematic of computational domain.

2. Numerical model and chemical mechanism

A commercially available program, CFD-ACE [22], was modified to incorporate detailed gas-phase and surface reaction mechanisms in CHEMKIN formats to simulate the flow and reaction characteristics inside a microchannel. For simplicity, the micro-reactor was modeled as a two-dimensional system with a gap width (L) of 1 mm between the two parallel plates in the numerical simulation. In practical applications, a micro-reactor with a large aspect ratio can be fabricated using MEMS technology. The numerical model consists of steady-state two-dimensional Navier–Stokes equations, mass and energy conservation equations, and a species equation for each chemical species.

Fig. 1 shows a schematic of the catalytic microchannel modeled in this work. Simulations were performed in one half of the microchannel due to symmetry. The computational domain contains both the gas-phase and the surrounding walls; the Fourier's heat conduction equation for the wall is solved simultaneously in order to better describe the surface reaction behavior. The reactor was 3 cm in length with a wall thickness of 0.4 mm. For the catalyst bed layout, most studies have used a single section of a uniform catalyst. Our previous study showed that catalyst segmentation obtains much better performance for the hydrogen/air reaction [23]. Therefore, the effects of the proposed design of catalyst segmentation and cavities on the enhancement of the methane/air catalytic reaction, which is slow in a catalyst bed, are studied in this paper. Cavities are also used primarily to enhance the residence time of the reactant mixture and reaction radicals generated from the upstream catalyst segment and to promote homogeneous reactions. A catalyst segment section in an inner wall of the micro-reactor was coated with a platinum catalyst. The total catalyst length was maintained at 1 cm for comparison with a single catalyst reactor. The length of one catalyst segment, the cavity width (w), and the cavity depth (d) are the variables used in this study.

The boundary conditions are as follows. The concentration of the methane/air mixture was specified at the inlet; the equivalence ratio was 0.6. The inlet temperature for the fuel–air mixture was preheated to 600 K for the proper light off of the fuel–air mixture on the catalyst. A uniform velocity profile was specified at the inlet and the flow field was laminar for all cases. The thermal condition at the wall was equivalent to the heat loss to the ambient air. The exterior heat loss was the heat convected by air, described by:

$$q'' = h\ (T_w - T_o) \quad (1)$$

where the heat transfer coefficient h equals 5 W/m^2/K in this study. T_w is the wall temperature and the ambient air temperature T_o is 300 K. At the exit, a constant pressure condition was specified with a constant ambient pressure of 101 kPa. An extrapolation scheme was used for species and temperature.

In the simulations, uniform meshes were used in the preliminary tests and non-uniform meshes with more grids clustered in the reaction region near the wall were used in subsequent runs to provide sufficient grid resolution in the computational domain. The number of grids depended on the channel dimensions. Grid independence was examined and a non-uniform mesh with a distribution of 211 × 65 grid points in the axial and transverse directions was used. The simulation was considered to converge when the residuals of all governing equations approached steady states. With

the convergence criteria, the results reported in this work have residuals smaller than 10^{-5}.

To obtain the gas properties and transport coefficients, the mixture density was first calculated using the ideal gas law. The mixture viscosity, specific heat, and thermal conductivity were then calculated from a mole fraction weighted average of species properties. Chemical reaction mechanisms were used in the gas-phase as well as on the catalyst surface of the inner wall. The reaction rate was represented by the modified Arrhenius expression; for heterogeneous reactions, all temperature exponents were set to zero. The GRI-Mech 3.0 mechanism, which comprises 53 species and 325 reaction steps, was first used for the homogeneous methane/air reaction. The simulation results were then compared with those from the skeletal mechanism, which comprises 9 species and 35 reaction steps [24]. The surface reaction mechanism was compiled primarily from that proposed by Deutschmann et al. [25]. These reaction mechanisms were used in previous studies; comparisons with experiment results are satisfactory [26,27]. For methane fuel, 11 surface species (C(s), CH(s), CH_2(s), CH_3(s), CO(s), CO_2(s), H(s), H_2O(s), O(s), OH(s), and PT(s)) describe the coverage of the surface with adsorbed species. PT(s) denotes free surface sites which are available for adsorption. The gas-phase chemical kinetics in CHEMKIN format and heterogeneous chemical kinetics in Surface CHEMKIN format were imported into the program. Details of the chemical reaction rate formulation and CHEMKIN format can be found in the user's manual [28,29].

3. Results and discussion

3.1. Kinetic validation

The skeletal kinetic mechanism can be used in simulations to significantly reduce computational time. Fig. 2 shows a comparison of the temperature and OH profiles along the plane of symmetry and OH mass fraction profiles along the wall for various kinetic mechanisms. The inlet velocity is 5 m/s and the wall thermal conductivity is 49 W/m/K. The axial profiles predicted using the GRI-Mech and skeletal mechanisms are quantitatively similar. Simulations were also performed for various inlet velocities and wall materials using the two reaction mechanisms. For the current numerical simulation cases, the skeletal model performs almost as well as the full reaction mechanism of GRI-Mech. Therefore, instead of using the time-consuming GRI-Mech 3.0 mechanism, the skeletal mechanism was used for subsequent studies of the effect of the proposed catalyst configuration on methane catalytic combustion in a microchannel.

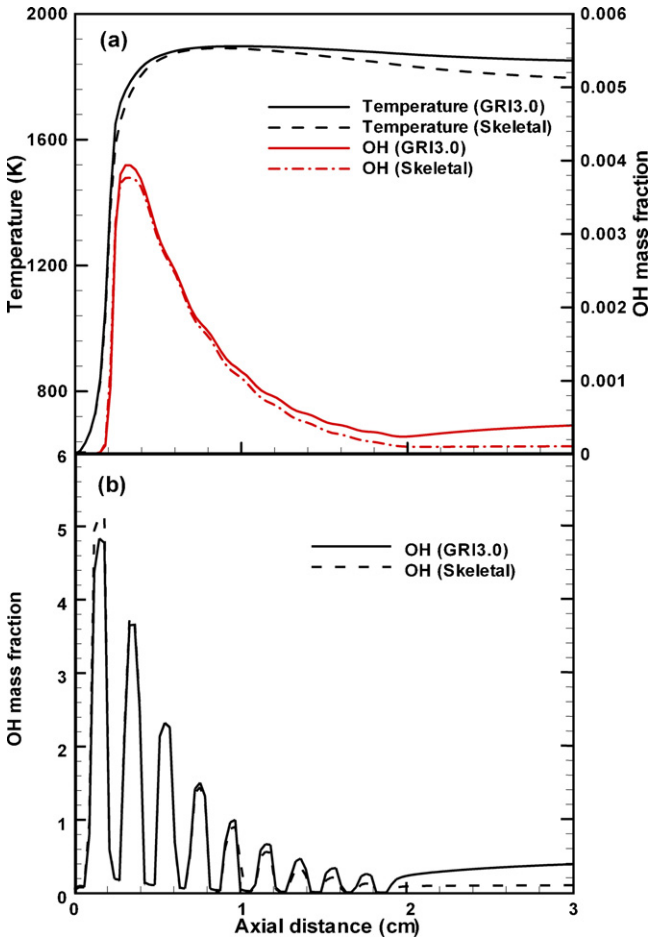

Fig. 2. Temperature and OH mass fraction for different mechanisms (a) along the plane of symmetry and (b) near the wall.

3.2. Combustion characteristics for various catalytic configurations

Platinum is widely utilized as a catalyst to enhance the lean reaction in micro-reactor systems. In general, catalytic combustion involves the coupling of the process of reactive flow and the process on the catalyst, leading to complex interactions between gas-phase (homogeneous) and surface (heterogeneous) reactions. The hetero-/homogeneous interaction becomes pronounced under high-velocity conditions. Well known aspects of this coupling include the promotion of gas-phase reactions due to catalytically induced exothermicity and the inhibition of gaseous reactions due to near-wall catalytic fuel depletion. Nevertheless, the hetero-/homogeneous radical coupling is weak in methane over PT [30,31]. Recent studies [26,30,31] have identified chemical coupling routes that are particularly relevant under micro-reactor conditions. The gas-phase combustion of methane can be roughly described by a two-step process: the incomplete oxidation of CH_4 to CO and the main heat-releasing oxidation of CO to CO_2. However, carbon monoxide has inherently active characteristics on the platinum surface due to its high sticking coefficient (0.85 on PT). By depriving CO from the gas-phase, the catalyst inhibits the onset of homogeneous ignition.

Although the gas-phase can still provide appreciable methane consumption without full flame formation via the incomplete oxidation of CH_4 to CO, the intensity of carbon monoxide concentration at the microchannel exit still increases under high-flow velocity conditions. In order to alleviate the problem of incomplete fuel conversion, catalyst segmentation is proposed to maintain the gas reaction in the micro-reactor for complete combustion within a specific distance. The principle of catalyst segmentation is to combine hetero- and homogeneous reactions to accomplish complete methane conversion, in contrast to the conventional catalyst configuration of radical competition between hetero- and homogeneous reactions. The cooperation between hetero- and homogeneous reactions is a two-stage process. First, the pre-reaction of the heterogeneous reaction on an upstream catalyst assists the downstream homogeneous reaction by providing sufficient catalytically induced exothermicity. The homogeneous reaction expedites the dissociation of fuel species, but the very short residence time leads to product-profound carbon monoxide in residual gas. Subsequently, the following sequentially-segmented catalyst inherits the heat and chemical radicals from upstream, and helps deplete carbon monoxide in the residual combustible mixture until complete conversion.

Fig. 3(a) shows the computed contours of CO_2, CO, and OH mass fractions and temperature distributions in the catalyst seg-

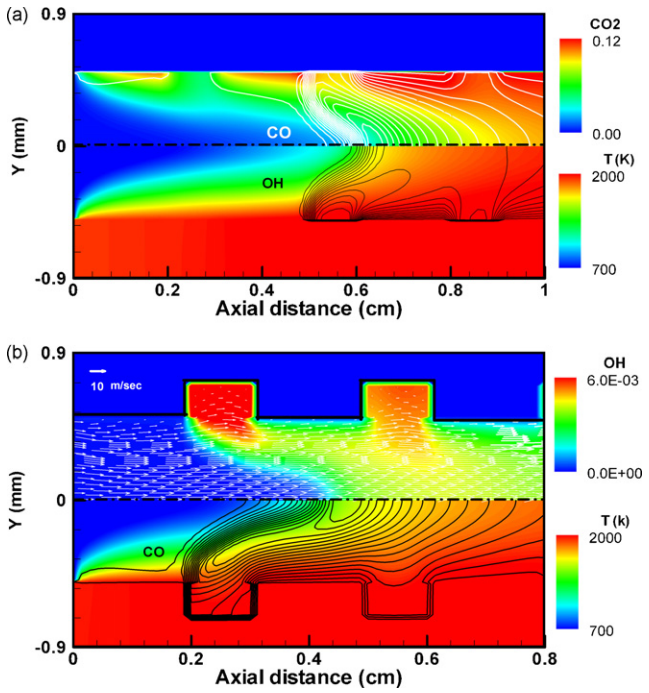

Fig. 3. (a) Contours of CO_2, CO and OH mass fraction as well as temperature in first 1.0 cm section of segmented catalyst and (b) contours of OH and CO mass fraction as well as temperature, and velocity distribution in first 0.8 cm section of segmented catalyst with cavities.

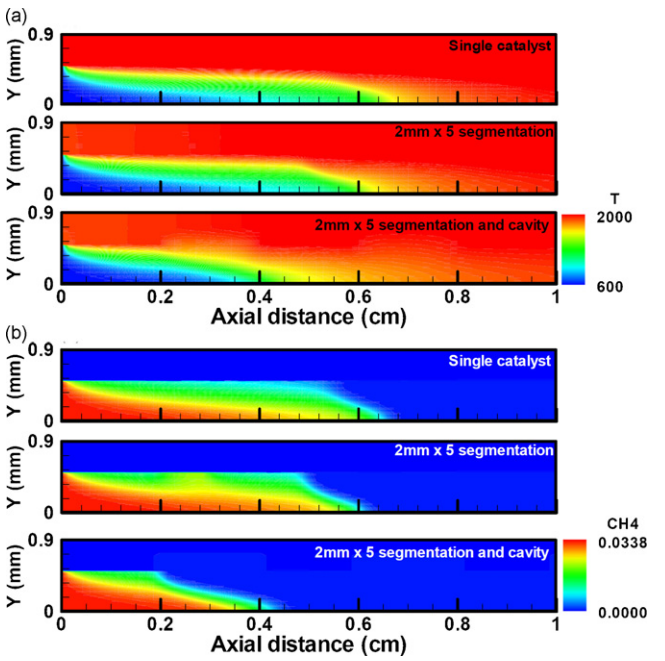

Fig. 4. Contours of (a) temperature and (b) methane mass fraction for different catalyst configurations, without segmentation and cavity, with 2 mm 5× segmentation, and with 2 mm 5× segmentation and cavity respectively.

mentation configuration. The simulation shows that the onset of heterogeneous reaction occurs in the first two catalyst segments. The pre-reaction increases the temperature of the combustible mixture and channel wall, and meantime some intermediate radicals are yielded. The space between adjacent segmented catalysts provides a proper dwelling place to sustain the homogeneous reaction with sufficient chemical radicals and catalytically induced exothermicity from upstream. The contour of OH mass fraction distribution in Fig. 3(a) shows that the location of the gas reaction is in the plane of symmetry of the channel, and that the flame is anchored on the inner wall. Furthermore, the contour of CO mass fraction in Fig. 3(a) shows the formation of carbon monoxide after the homogeneous reaction; a considerable amount of carbon monoxide is consumed on the following catalyst surface.

The proposed catalyst segmentation effectively integrates hetero- and homogeneous reactions to accomplish complete methane conversion in a micro-reactor. However, flame anchoring is affected by flow velocity. High inlet velocity may reduce the residence time and defer the onset of homogeneous ignition downstream. In order to enhance flame stabilization in the micro-reactor, localized cavities on the channel wall are proposed. The main function of cavities is to provide a low-velocity zone to stabilize the homogeneous reaction. Fig. 3(b) shows the contours of OH and CO mass fractions, and the temperature and velocity distributions in the first 0.8-cm section of the segmented catalyst and cavities. Results show that the magnitude of flow velocity inside the cavities is relatively low compared to that in the main stream; cavities thus enhance the stabilization of homogeneous reactions by providing a low-velocity asylum. The distribution of the CO mass fraction shows the pre-reaction of the fuel mixture in an upstream catalyst segment; the congregation of OH radicals in the cavities represents flame anchoring. The flame anchoring location is upstream of that shown in Fig. 3(a).

Three kinds of micro-reactor design were investigated, i.e., a system with a single catalyst, a system with catalyst segmentation, and a system with catalyst segmentation and cavities. Fig. 4 shows the computed temperature and methane mass fraction contours for the three catalyst configurations in the first 1-cm section. Fig. 5 shows OH mass fraction contours for the whole section. The equivalence ratio of these cases is 0.6 and the inlet velocity is 10 m/s. The wall thermal conductivity was fixed at 49 W/m/K unless otherwise indicated. This velocity substantially surpasses the flame speed of methane; homogeneous combustion cannot exist in a micro-reactor with non-catalytic walls under this condition. However, the catalyst on the wall evidently extended the blowout limit of methane.

Numerical results indicate that homogeneous combustion occurred in the plane of symmetry for all cases, and that their corresponding flame anchoring positions are different, as shown in the high OH concentration regions in Fig. 5. In the single catalyst case, some fuel was consumed by heterogeneous reactions in the vicinity of the catalyst surface and some fuel was consumed by homogeneous reactions in the central region. The catalytic surface supplies heat, radicals, and bare active site; it thus sustains the gas reaction in this region. This is a conventional case of catalytically-stabilized homogeneous combustion.

For the multi-segment catalyst, the homogeneous combustion was sustained in the spaces between catalyst segments, where

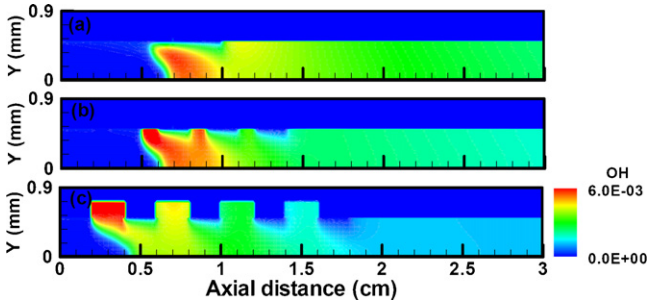

Fig. 5. Contours of OH mass fraction for different catalyst configurations: (a) without segmentation and cavity, (b) with 2 mm 5× segmentation, and (c) with 2 mm 5× segmentation and cavity.

the mixture inherits prior catalytically induced exothermicity and chemical radicals. High-flow velocity makes the flame anchor downstream of the second catalyst segment. The catalyst segmentation in Fig. 4(b) indicates that methane depletion occurs within the first two catalyst segments, and that surface chemistry dominates the local reaction in this region. Subsequently, a large amount of radicals congregates on the non-catalyst wall, where homogeneous chemistry dominates the local reaction, as shown in Fig. 5(b). For multi-segment catalyst and cavities, methane is completely consumed in a short distance and the flame anchor moves upstream under the high velocity condition, as shown in Fig. 5(c). This configuration can thus substantially reduce the dimensions of the micro-reactor and lower the amount of required catalyst material. The performance of the integrated catalyst segmentation and interlacing cavities on channel walls is superior to that of the single catalyst, especially for high-velocity flows. The effects of catalyst layout, cavity configuration, reactor properties are discussed below.

3.3. Combustion characteristics under various catalyst layouts

As described above, catalyst segmentation and cavities improve combustion and enhance the flame stability in a micro-reactor. The effects of catalyst layout and cavity configuration are described in this section. Fig. 6(a) shows the fuel mass fraction along the plane of symmetry. Four types of catalyst layout were considered: 1-mm catalyst with 10 segments, 2-mm catalyst with five segments, 5-mm catalyst with two segments, and 10-mm catalyst without segmentation. Fig. 6(b) shows the OH mass fraction distributions along the axial direction near the inner wall. The length of the catalyst gap (non-catalyst wall) between two segments was fixed 1 mm for all cases. For the single catalyst case, 10-mm PT in length, the fuel consumption had two distinct characteristics. The first smooth decline region is caused by catalytic combustion and it is obvious under the kinetically controlled region. The reaction in the catalyst section was slow and limited by the catalytic reaction and wall temperature, which led to a relatively low fuel consumption rate. Subsequently, the fuel concentration abruptly declines at the axial distance of approximate 6.5 mm from the inlet due to the homogeneous reaction in this section.

For the multi-segment catalyst case, the amount of fuel is significantly decreased at the first catalyst gap except for the case of 1-mm PT with 10 segments. Methane consumption occurred within the first two catalyst segments, and significantly declined at the axial distance of approximate 4 mm in the channel for the 1-mm PT-10 segments case. The homogeneous reaction was postponed until the second catalyst segment because a short catalyst segment cannot sustain the heterogeneous reaction due to the short residence time and high heat loss under high velocity conditions. The homogeneous reaction was thus postponed until sufficient heat and radicals accumulated. For the cases of 2-mm PT with five segments and 5-mm PT with two segments, the kinetic controlled region curtails compared to the single catalyst case, and the onset of homogeneous reaction moves upstream in the first catalyst gap. High OH concentration peaks emerge in each catalyst gap, as shown in Fig. 6(b). Consequently, a proper catalyst length must be taken into consideration based on the range of flow velocity and fuel concentration.

In order to further verify the effect of cavity configuration on the chemical reaction, the depth and width of the cavity were considered for the 2-mm PT with five segments case. Fig. 7 shows the contours of OH and CO mass fractions for cavity widths of $w = 1$, 2, and 3 mm under a fixed flow velocity (10 m/s) and equivalence ratio ($\Phi = 0.6$). The pre-reaction of methane in the first catalyst segment delivers radicals and heat to the first cavity, and promotes the homogeneous reaction in the cavity for the cases of $w = 1$ and 2 mm. OH concentration distribution reveals that OH radicals concentrate in the first cavity, indicating that the homoge-

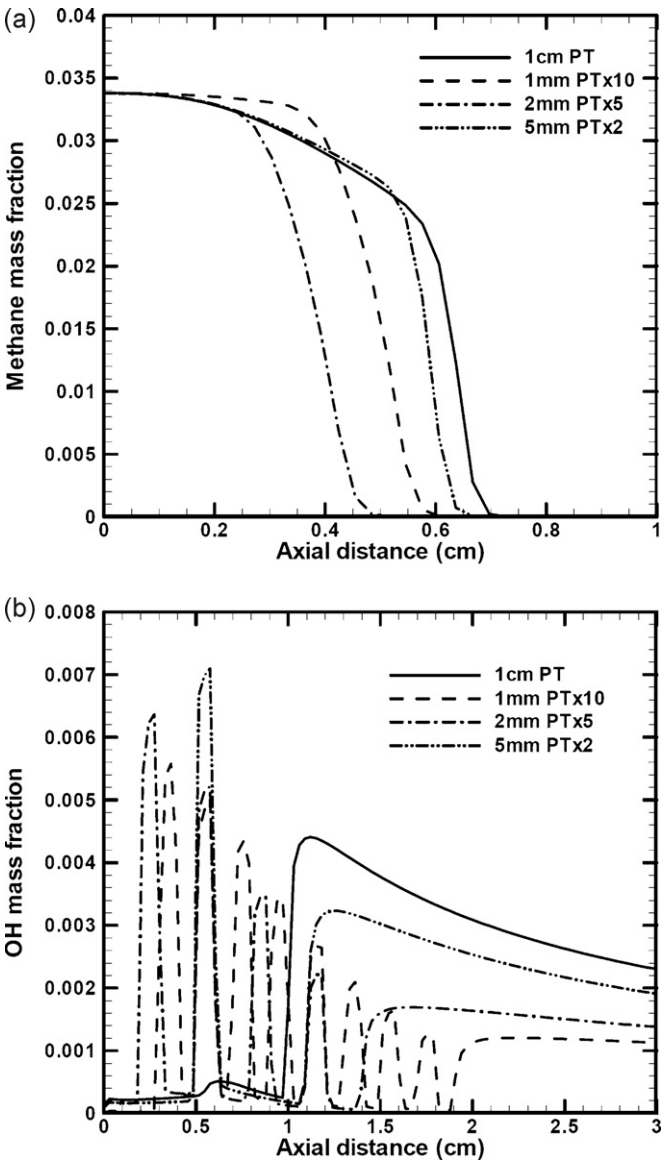

Fig. 6. (a) Methane mass fractions along the plane of symmetry and (b) OH mass fractions near the wall for different catalyst segmentations.

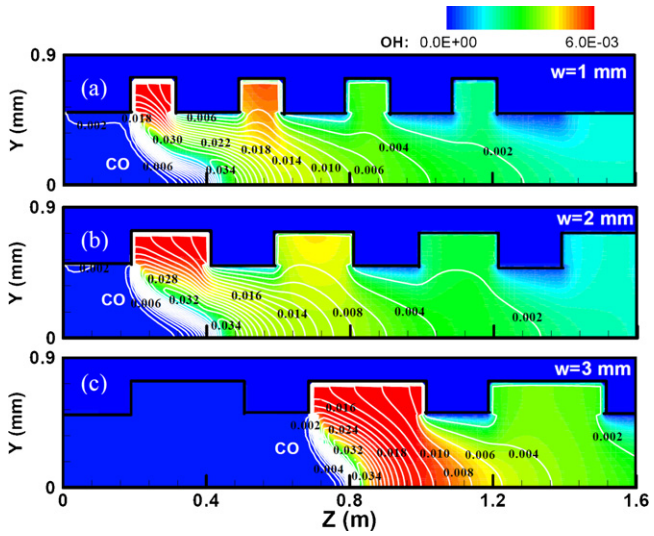

Fig. 7. Contours of OH and CO mass fraction for different cavity widths: (a) 1 mm, (b) 2 mm and (c) 3 mm.

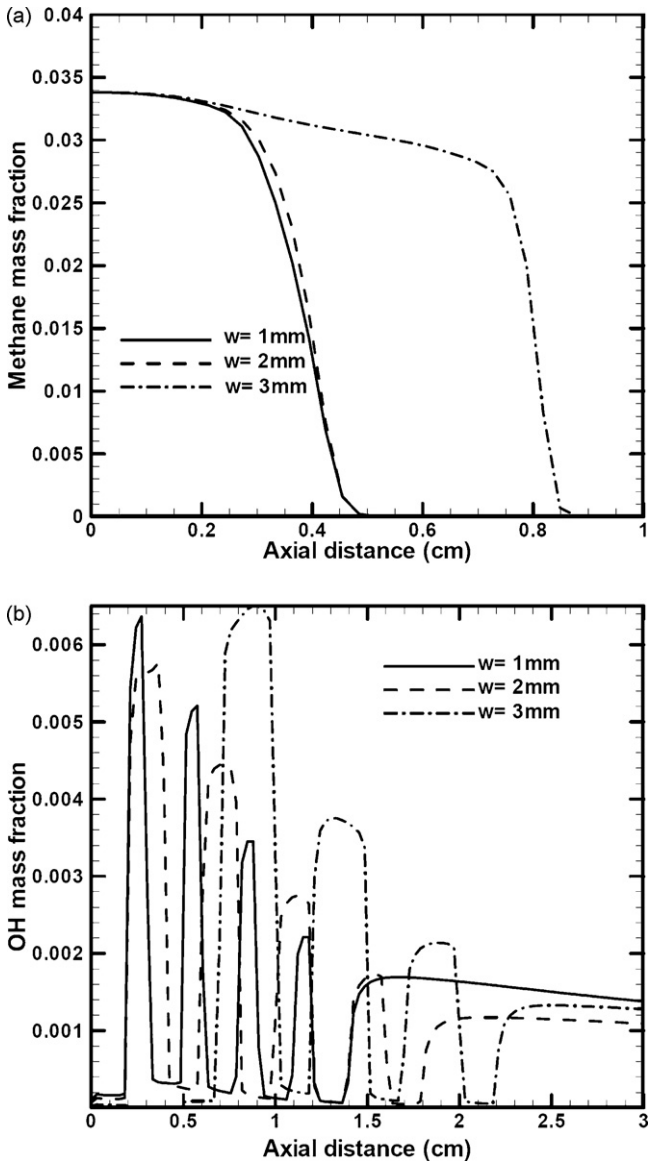

Fig. 8. Methane mass fractions along the plane of symmetry, and OH mass fractions near the wall for different cavity widths.

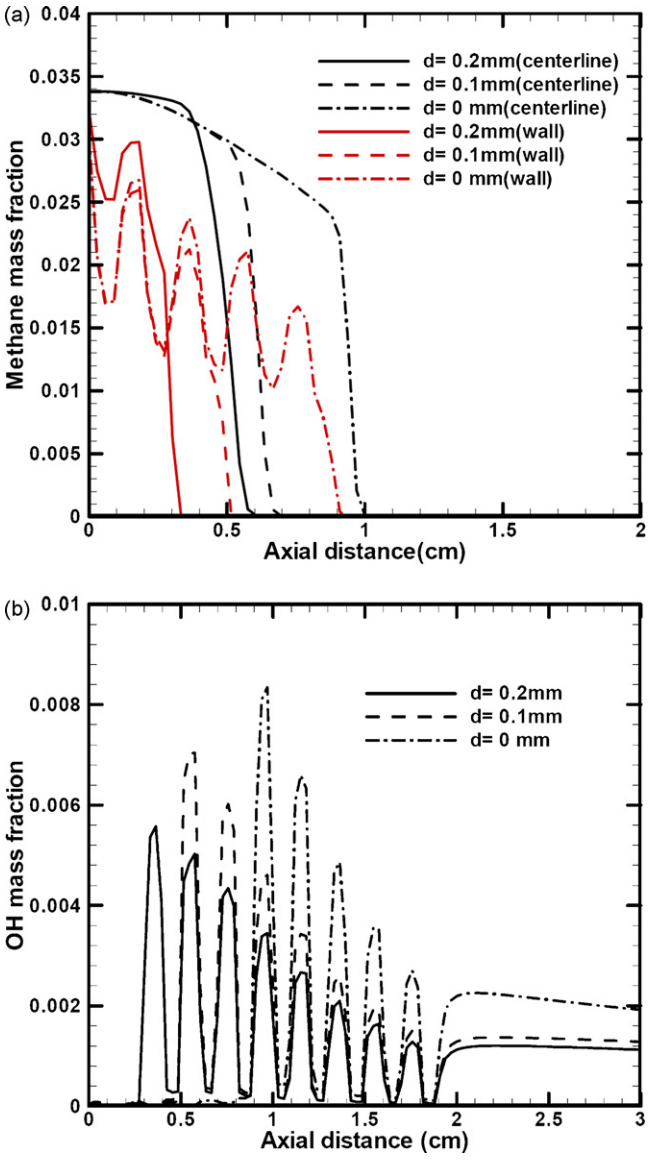

Fig. 9. (a) Methane mass fractions along the plane of symmetry and near the wall and (b) OH mass fractions near the wall for different cavity depths.

neous reaction and flame anchoring occurs there. The large amount of CO formation after the homogeneous reaction is due to incomplete combustion; the formation becomes depleted in the following catalyst segments. For the case of $w = 3$ mm, there is no homogeneous reaction in the first cavity, resulting in radical quenching on the non-catalyst wall. The excessively large width of the wall cavity may impede heat conduction via the wall, and thus reduce wall temperature. This postpones the ignition of the homogeneous reaction in the second cavity in the case of $w = 3$ mm, as shown in Fig. 7(c).

The methane mass fraction along the plane of symmetry and OH mass fraction near the wall for the three catalyst widths are shown in Fig. 8. Fig. 8(a) shows that the distance required to reach complete methane conversion in the cases of $w = 1$ and 2 mm is half that for the case of $w = 3$ mm. Fig. 8(b) shows that there is a high OH concentration in the first cavity in the cases of $w = 1$ and 2 mm, but that no OH radicals exist in the first cavity for the case of $w = 3$ mm. Therefore, the cavity width must be selected to minimize the blockage of thermal conduction via the wall while maximizing the cavity space to collect sufficient radicals.

Cavity depth is another essential parameter. Cavity depths of $d = 0$, 0.1, and 0.2 mm under the conditions of $w = 1$ mm, 2-mm PT with 5 segments, and a flow velocity of 10 m/s were examined. Fig. 9(a) shows the methane fractions along the plane of symmetry and near the wall for the three cavity depths. Results show that methane is consumed in the catalyst gaps. The micro-reactor with cavities ($d = 0.1$ and 0.2 mm) requires a shorter distance for complete methane conversion compared to the case without cavities ($d = 0$ mm). The case with $d = 0.2$ mm has less methane consumption in the first catalyst segment, but it has almost complete methane consumption in the second cavity segment due to the rapid homogeneous reaction. The case with $d = 0.2$ mm has relatively large methane consumption compared to the case with $d = 0.1$ mm. The large cavity depth impedes downstream exothermic heat from conducting upstream, which decreases the heterogeneous reaction of the catalyst in the upstream region.

Fig. 9(b) shows the OH mass fraction near the wall for the three cavity depths. The onset of the homogeneous reaction in the case with a large depth ($d = 0.2$ mm) was upstream of those of the other cases. The large cavity depth captures more

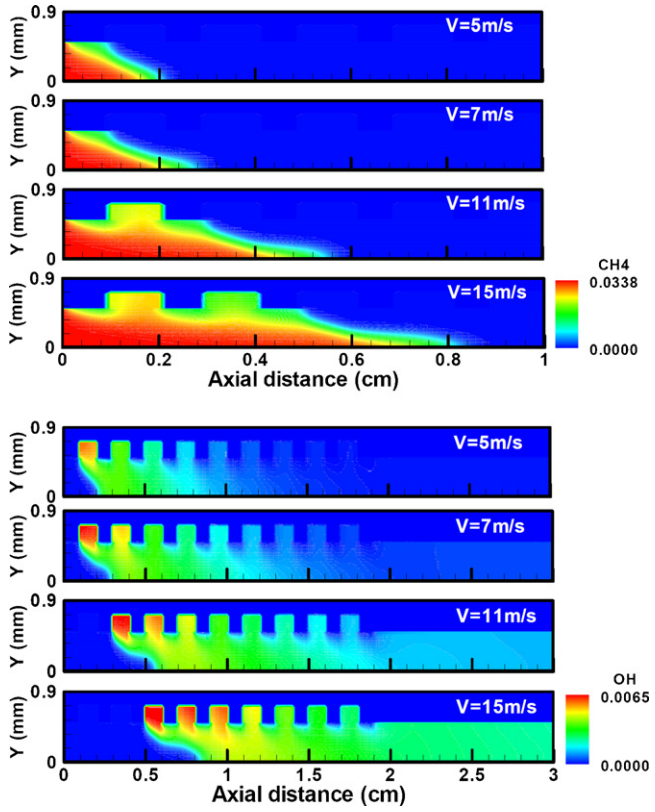

Fig. 10. (a) Contours of CH_4 mass fraction and (b) OH mass fraction for different inlet velocities.

radicals from upstream, increases the contact surface of the high-temperature wall, and enhances the residence time of the combustible mixture in the cavity, thus enhancing the homogeneous reaction in the cavity. However, increasing the depth of the cavity means increasing the thickness of the micro-reactor and increasing the heat loss through the wall. An appropriate combination of cavity width and depth leads to high overall fuel conversion.

3.4. Combustion characteristics under various flow conditions

To further examine the operational characteristics of a multi-segment catalyst and cavities in a micro-reactor, the effects of inlet velocity are considered in this section. Fig. 10 shows contours of methane and OH mass fraction for various inlet velocities for 1-mm PT with 10 segments and 0.2 mm (d) × 1 mm (w) cavities. The inlet velocity was varied from 5 to 15 m/s. For smaller inlet velocities (5 and 7 m/s), methane was completely depleted within a short distance of 2 mm from the entrance, and homogeneous combustion occurred near the entrance.

Depending on the inlet velocity, multi-segment catalyst and cavities gradually underscores the specific effects on enhancing and sustaining homogeneous combustion inside the catalytic micro-reactor. Increasing the flow rate leads to a shorter residence time, which is detrimental for a complete reaction, but the existence of the cavities will enhance the reaction and maintain homogeneous combustion in the cavity. As shown in Fig. 10(b), the OH concentration distribution recedes downstream depending on the inlet flow. Catalyst segmentation and cavities in the micro-reactor extends the flammability limit of a small-scale system for a wide variety of inlet velocities, and controls the location of the flame anchoring and heat source in the micro-reactor system.

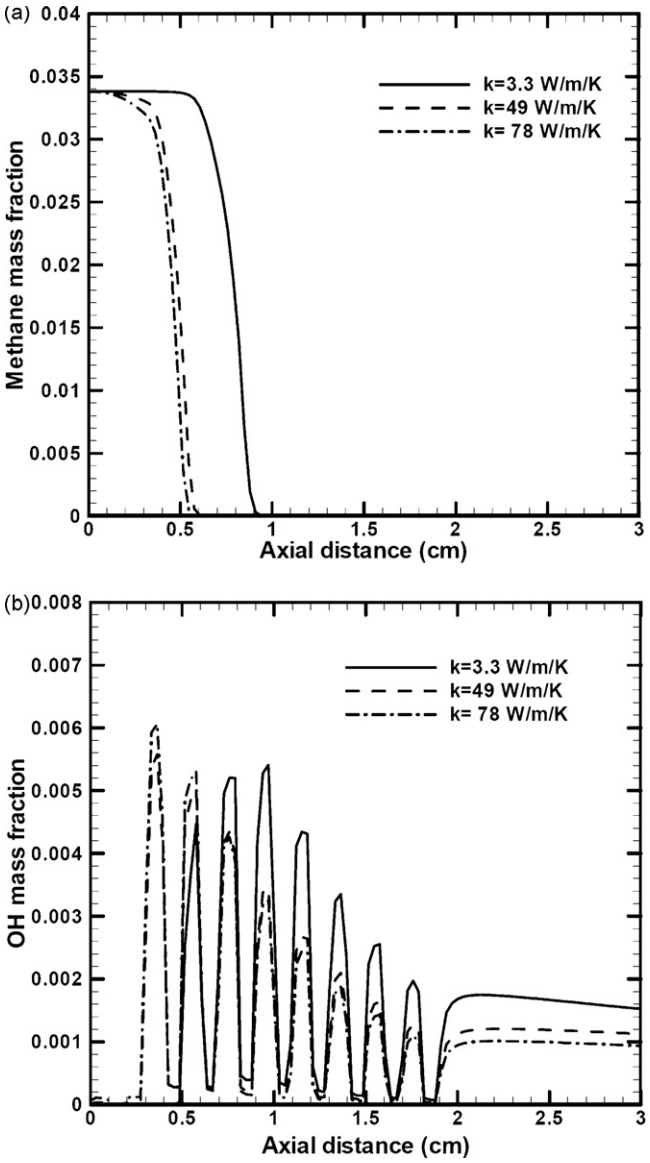

Fig. 11. (a) Methane mass fractions along the plane of symmetry and (b) OH mass fractions near the wall for different thermal conductivity effects.

3.5. Combustion characteristics under various reactor properties

The thermal conductivity of the wall material affects the chemical effectiveness of hetero- and homogeneous reactions in the micro-reactor. Therefore, three kinds of material appropriate for application in MEMS manufacturing are considered here, i.e., cordierite (k = 3.3 W/m/K), steel (k = 49 W/m/K), and platinum (k = 78 W/m/K), to further examine the effect of the thermal conductivity on the proposed catalyst configuration. Fig. 11 shows methane mass fractions along the plane of symmetry, and OH mass fractions near the wall for the three wall materials. In all cases, the multi-segment catalyst layout is 2-mm PT with 5 segments and the cavity dimensions are 0.2 mm (d) by 1 mm (w). The inlet velocity is 10 m/s and the corresponding equivalence ratio is 0.6. Results indicate that the methane conversion for the system with a relatively large thermal conductivity is quicker than that for the system with a relatively small one.

The homogeneous reaction in the cases of large thermal conductivity (k = 49 and 78 W/m/K) occurs in the first cavity. In contrast, the onset of the homogeneous reaction in the case of low ther-

mal conductivity (k = 3.3 W/m/K) occurs in the second cavity. Large thermal conductivity allows catalytically induced exothermicity to be delivered to the whole system via the wall, so that sufficient wall temperature can induce homogeneous combustion in the upstream cavity. However, large thermal conductivity increases the heat loss through the wall. Metallic support is an appropriate material for fabricating multi-segment catalyst micro-reactors with cavities due to its easy-machining and high thermal conductivity.

4. Conclusion

The proposed multi-segment catalyst with cavities for a micro-reactor was investigated using numerical simulation with detailed hetero- and homogeneous chemistries of methane/air reactions. The combustion characteristics of the multi-segment catalyst with cavities were categorized and discussed in terms of catalyst lay-out, cavity dimensions, flow conditions, and reactor properties. Results reveal that the pre-reaction of the heterogeneous reaction in the upstream catalyst segment can produce active chemical radicals and catalytically induced exothermicity; the homogeneous reaction is subsequently induced and anchored in the cavity. Carbon monoxide was massively discharged after the homogeneous reaction due to incomplete combustion. The downstream catalyst segments fully consume carbon monoxide due to the preferred CO catalytic reaction of the high sticking coefficient on the platinum surface. This process of methane catalytic combustion belongs to mutual assisting coupling between the hetero- and homogeneous reactions, instead of the mutual competition in a conventional catalyst reactor. Full methane conversion and complete combustion can thus be accomplished in a short distance, allowing the system to be further scaled down. Cavities appreciably extend the stable operation range of the micro-reactor for a wide variety of inlet flow velocities. The proposed catalyst configuration can thus be used in various small-scale power/heating generation systems.

Acknowledgment

Computer time and numerical packages provided by the National Center for High-Performance Computing, Taiwan (NCHC-Taiwan), are acknowledged.

References

[1] D. Dunn-Rankin, E.M. Leal, D.C. Walther, Prog. Energy Combust. Sci. 31 (2005) 422–465.
[2] M.-H. Wu, Y. Wang, V. Yang, R.A. Yetter, Proc. Combust. Inst. 31 (2007) 3235–3242.
[3] N.O. Moraga, C.E. Rosas, V.I. Bubnovich, N.A. Solari, Int. J. Heat Mass Transfer 51 (2008) 302–311.
[4] Y.-H. Li, Y.-C. Chao, N.S. Amadé, D. Dunn-Rankin, Exp. Thermal Fluid Sci. 32 (2008) 1118–1131.
[5] Y.-H. Li, Y.-S. Lien, Y.-C. Chao, D. Dunn-Rankin, Prog. Photovolt.: Res. Appl. 17 (2009) 327–336.
[6] T.L. Marbach, V. Sadasivuni, A.K. Agrawal, Combust. Sci. Technol. 179 (2007) 1901–1922.
[7] W.A. Sirignano, T.K. Pham, D. Dunn-Rankin, Proc. Combust. Inst. 29 (2002) 925–931.
[8] A.C. Fernandez-Pello, Proc. Combust. Inst. 29 (2003) 883–889.
[9] A. Mehra, X. Zhang, A.A. Ayon, I.A. Waitz, M.A. Schmidt, C.M. Spadaccini, J. Microelectromech. Syst. 9 (2000) 517–527.
[10] P.D. Ronney, Combust. Flame 135 (2003) 421–439.
[11] N.I. Kim, S. Kato, T. Kataoka, T. Yokomori, S. Maruyama, T. Fujimori, K. Maruta, Combust. Flame 141 (2005) 229–240.
[12] S. Yuasa, K. Oshimi, H. Nose, Y. Tennichi, Proc. Combust. Inst. 30 (2005) 2455–2462.
[13] O. Demoulin, B.L. Clef, M. Navez, P. Ruiz, Appl. Catal. A 344 (2008) 1–9.
[14] S.J. Volchko, C.-J. Sung, Y. Huang, S.J. Schneider, J. Propul. Power 22 (2006) 684–693.
[15] O. Demoulin, M. Navez, P. Ruiz, Appl. Catal. A 295 (2005) 59–70.
[16] K. Maruta, K. Takeda, J. Ahn, K. Borer, L. Sitzki, P.D. Ronney, O. Deutschmann, Proc. Combust. Inst. 29 (2002) 957–963.
[17] S. Raimondeau, D.G. Norton, D.G. Vlachos, R.I. Masel, Proc. Combust. Inst. 29 (2002) 901–907.
[18] D.G. Norton, D.G. Vlachos, Chem. Eng. Sci. 58 (2003) 4871–4882.
[19] D.G. Norton, D.G. Vlachos, Combust. Flame 138 (2004) 97–107.
[20] J. Hua, M. Wu, K. Kumar, Chem. Eng. Sci. 60 (2005) 3497–3506.
[21] N.S. Kaisare, D.G. Vlachos, Catal. Today 120 (2007) 96–106.
[22] CFD-ACE, CFDRC, Huntsville, AL, 2003.
[23] G.-B. Chen, Y.-C. Chao, C.-P. Chen, Int. J. Hydrogen Energy 33 (2008) 2586–2595.
[24] M.D. Smooke, Lecture Notes in Physics, vol. 384, Springer-Verlag, 1991, pp. 137–158.
[25] O. Deutschmann, R. Schmidt, F. Behrendt, J. Warnatz, Proc. Combust. Inst. 26 (1996) 1747–1754.
[26] S. Karagiannidis, J. Mantzaras, G. Jackson, K. Boulouchos, Proc. Combust. Inst. 31 (2007) 3309–3317.
[27] O. Deutschmann, L.I. Maier, U. Riedel, A.H. Stroemman, R.W. Dibble, Catal. Today 59 (2000) 141–150.
[28] R.J. Kee, F.M. Rupley, E. Meeks, J.A. Miller, Chemkin-III: A Fortran Chemical Kinetics Package for the Analysis of Gas Phase Chemical and Plasma Kinetics, Sandia National Laboratories Report SAND96-8216, 1996.
[29] M.E. Coltrin, R.J. Kee, F.M. Rupley, E. Meeks, Surface-Chemkin-III: A Fortran Package for Analyzing Heterogeneous Chemical Kinetics at a Solid-Surface–Gas-Phase Interface, Sandia National Laboratories Report SAND96-8217, 1996.
[30] M. Reinke, J. Mantzaras, R. Schaeren, R. Bombach, A. Inauen, S. Schenker, Combust. Flame 136 (2004) 217–240.
[31] M. Reinke, J. Mantzaras, R. Bombach, S. Schenker, A. Inauen, Combust. Flame 141 (2005) 448–468.